Luteolin enhances drug chemosensitivity by downregulating the FAK/PI3K/AKT pathway in paclitaxel-resistant esophageal squamous cell carcinoma

ZHENZHEN YANG[1,2], HONGTAO LIU[3], YINSEN SONG[1], NA GAO[1,2], PAN GAO[1,2], YIRAN HUI[2,4], YUEHENG LI[2] and TIANLI FAN[2]

[1]The Fifth Clinical Medical College of Henan University of Chinese Medicine (Zhengzhou People's Hospital), Zhengzhou, Henan 450003, P.R. China; [2]School of Basic Medical Sciences, Zhengzhou University, Zhengzhou, Henan 450001, P.R. China; [3]School of Life Sciences, Zhengzhou University, Zhengzhou, Henan 450001, P.R. China; [4]University of Chinese Academy of Sciences Shenzhen Hospital, Shenzhen, Guangdong 518107, P.R. China

Received March 28, 2024; Accepted June 12, 2024

DOI: 10.3892/ijmm.2024.5401

Abstract. Drug resistance is a key factor underlying the failure of tumor chemotherapy. It enhances the stem-like cell properties of cancer cells, tumor metastasis and relapse. Luteolin is a natural flavonoid with strong anti-tumor effects. However, the mechanism(s) by which luteolin protects against paclitaxel (PTX)-resistant cancer cell remains to be elucidated. The inhibitory effect of luteolin on the proliferation of EC1/PTX and EC1 cells was detected by cell counting kit-8 assay. Colony formation and flow cytometry assays were used to assess clonogenic capacity, cell cycle and apoptosis. Wound healing and Transwell invasion tests were used to investigate the effects of luteolin on the migration and invasion of EC1/PTX cells. Western blotting was used to detect the protein levels of EMT-related proteins and stem cell markers after sphere formation. Parental cells and drug-resistant cells were screened by high-throughput sequencing to detect the differential expression of RNA and differential genes. ELISA and western blotting were used to verify the screened PI3K/Akt signaling pathway, key proteins of which were explored by molecular docking. Hematoxylin and eosin staining and TUNEL staining were used to observe tumor xenografts on morphology and apoptosis in nude mice. The present study found that luteolin inhibited tumor resistance (inhibited proliferation, induced cell cycle arrest and apoptosis and hindered migration invasion, EMT and stem cell spherification) *in vitro* in PTX-resistant esophageal squamous cell carcinoma (ESCC) cells. In addition, luteolin enhanced drug sensitivity and promoted the apoptosis of drug-resistant ESCC cells in combination with PTX. Mechanistically, luteolin may inhibit the PI3K/AKT signaling pathway by binding to the active sites of focal adhesion kinase (FAK), Src and AKT. Notably, luteolin lowered the tumorigenic potential of PTX-resistant ESCC cells but did not show significant toxicity *in vivo*. Luteolin enhanced drug chemosensitivity by downregulating the FAK/PI3K/AKT pathway in PTX-resistant ESCC and could be a promising agent for the treatment of PTX-resistant ESCC cancers.

Correspondence to: Professor Tianli Fan, School of Basic Medical Sciences, Zhengzhou University, 100 Science Avenue, Zhengzhou, Henan 450001, P.R. China
E-mail: fantianli@zzu.edu.cn

Key words: luteolin, esophageal squamous cell carcinoma, drug chemosensitivity, molecular docking, focal adhesion kinase/PI3K/AKT pathway

Introduction

Esophageal cancer (EC) is one of the most common and lethal malignant tumors of the digestive tract (1). It is characterized by aggressive metastasis, which leads to a poor prognosis and low 5-year survival rates (2). Esophageal squamous cell carcinoma (ESCC) is a common histopathological subtype worldwide and is estimated to account for 90% of EC cases in China (3-4). According to the specific stage of the disease, treatment methods primarily include surgery, chemotherapy and radiotherapy. However, despite thorough investigations by the research community, the prognosis of the disease has not improved markedly in the past 20 years and the disease currently has a 5-year survival rate of <20% (5-6).

Thus far, combined chemotherapy before ESCC surgery has proven to be beneficial (7-9). Cisplatin (DDP) and paclitaxel (PTX) are promising chemotherapeutics that are increasingly being used in ESCC treatment (10). However, a large proportion of patients do not respond positively to chemotherapy and exhibit severe side effects (i.e. bone marrow suppression, allergic reactions, nausea and vomiting and cardiotoxicity), which could potentially lead to resistance and recurrence (11). Therefore, it is necessary to screen appropriate combination reagents to address issues of drug resistance and enhance the sensitivity of ESCC to anticancer therapy.

Multi-drug resistance (MDR) is a key factor responsible for the failure of tumor chemotherapy, usually because the

increase in drug outflow leads to a decrease in drug accumulation in tumor cells (12). Luteolin, as one of the most common flavonoid compounds, is widely present in a number of plants, such as mint, rosemary, thyme, pine and ferns (13). A previous published article have shown that luteolin sensitizes DDP-resistant ovarian cell lines and xenograft models by inducing apoptosis and inhibiting cell migration and invasion (14). Luteolin also increases the sensitivity of cells by inhibiting the Nrf2 pathway in oxaliplatin-resistant colorectal cancer cells (15). Another study reported that luteolin enhances the accumulation of p53 and promotes the therapeutic activity of cisplatin in ovarian cancer cells in a mouse xenograft model *in vivo* (16). These results indicate the potential chemosensitivity of various cancer cells to luteolin and the applicability of luteolin as an adjuvant in the regulation of drug sensitivity. However, only a few reports have been published on whether luteolin can increase chemotherapeutic sensitivity in PTX-resistant ESCC and the potential mechanism involved. This topic warrants further research.

The current study investigated the bio-functions of luteolin in the PTX-resistant esophageal squamous cell line EC1/PTX and the chemosensitizing effects of luteolin combined with PTX EC1/PTX *in vitro* and *in vivo*. It also explored the associated molecular mechanisms based on the findings.

Materials and methods

Cell lines and cell culture. ESCC cells (EC1) were obtained from the Cell Bank of Type Culture Collection of The Chinese Academy of Sciences. PTX-resistant cell lines EC1/PTX (17) were established by our group. Cells from the two ESCC cell lines were cultured in RPMI-1640 (Gibco; Thermo Fisher Scientific, Inc.) supplemented with 10% fetal bovine serum (FBS; Gibco; Thermo Fisher Scientific, Inc.). Cells were incubated at 37˚C in the presence of 5% CO_2.

Cell counting kit-8 (CCK-8) assay. A total of $3x10^3$ cells/ml were seeded in 96-well culture plates with five replicate wells in each group. PTX (6 mg/ml) or luteolin (120 mmol/l) was used to treat the cells for 24 or 48 h. Subsequently, according to the manufacturer's instructions, 10 μl of CCK-8 reagent (Dojindo Molecular Technologies, Inc.) was added to each well and the cells were incubated for another 3 h at 37˚C. Cell viability was determined based on the optical density at 450 nm measured using a microplate reader (Victor1420; PerkinElmer, Inc.). The experiment was performed at least three times and in triplicate.

Colony formation assay. A total of $2x10^3$ cells/ml were seeded in a six-well plate. In each well, 0.1% DMSO and 10, 20, or 40 μM luteolin were added. The cells were incubated at 37˚C for 7 days. In accordance with the manufacturer's instructions, the cells were fixed with 1 ml of 4% paraformaldehyde for 30 min and stained with 1% crystal violet for 30 min at room temperature. The number of colonies formed was then determined. Experiments were repeated at least three times.

Flow cytometry assay. For tests on apoptosis, an Annexin V-FITC apoptosis detection kit (BD Biosciences) was used according to the manufacturer's instructions. EC1/PTX cells were treated with luteolin at different concentrations (10, 20, or 40 μM) for 24 h. Further, cells were stained with 5 μl of Annexin-FITC and 10 μl of PI and kept for 15 min in the dark at room temperature. FlowJo 7.6 (FlowJo LLC) software was used to analyze data. Early apoptotic cells (Annexin V-positive and PI-negative) and late apoptotic cells (Annexin V-positive and PI-positive) were both included while calculating the apoptosis rate. Experiments were performed in triplicate. Iced PBS was used to wash the cells in the cell cycle distribution assay. Following this, the cells were fixed in ethanol at -20˚C. This was followed by re-suspension of the cells in PBS and treatment with 40 μg/ml PI, 0.1 mg/ml RNase A and 0.1% Triton X-100 for 30 min in a dark room at 37˚C. Then, the cells were analyzed using flow cytometry.

Wound healing. The wound healing assay was conducted in accordance with a previously published method (18) with minor modifications. Briefly, ESCC cells adherent in 35 mm dishes were scratched with 10 μl pipette tips and washed twice with PBS. Following this, 0.1% DMSO and 10 μM or 20 μM luteolin were added to each well. The cells were incubated overnight in serum-free medium at 37˚C in the presence of 5% CO_2. ImageJ v1.8.0 software (National Institutes of Health) was used to calculate the area of scratches and analyze cell mobility in the different treatment groups.

Transwell assay. Serum-free Opti-Minimum Essential Medium (MEM; Invitrogen; Thermo Fisher Scientific, Inc.) was used to resuspend cells at a density of $3x10^4$ cells/ml. Next, 50 μl of Matrigel (Millipore Sigma) was spread in the chamber and 600 μl of 10% RPMI-1640 medium was added dropwise to the basolateral chamber under 37˚C within 1 h. The chambers were immersed 4% paraformaldehyde for 30 min and stained with 1% crystal violet for 1 h at room temperature. The number of stained cells was counted using an inverted microscope.

Western blotting. RIPA lysis buffer (Cell Signaling Technology, Inc.) was used to isolate total protein from the cells. A BCA protein assay kit (Thermo Fisher Scientific, Inc.) was used to measure the protein concentration according to the manufacturer's instructions. Then, 50 μg of protein was separated using 10% sodium dodecyl sulfate-polyacrylamide gel electrophoresis (SDS-PAGE) and transferred to polyvinylidene fluoride membranes. The membranes were subsequently blocked with 5% non-fat milk for 2 h at 37˚C. This was followed by overnight treatment with primary antibodies against N-cadherin (1:5,000; cat. no. ab76011; Abcam), MMP-2 (1:1,000; cat. no. ab92536; Abcam), Snail (1:1,000; cat. no. ab216347; Abcam), CD133 (1:2,000; cat. no. Ab222782; Abcam), CD44 (1:1,000; cat. no. ab243894; Abcam), sex determining region Y-box 2 (SOX-2) (1:1,000; cat. no. Ab92494; Abcam), AKT (1:1,000; cat. no. ab8805; Abcam), phosphorylated (p-)AKT (1:5,000; cat. no. ab81283; Abcam), Src (1:1,000; cat. no. 2109; Cell Signaling Technology), p-Src (1:1,000; cat. no. 59548; Cell Signaling Technology), epidermal growth factor receptor-2 (ErbB2) (1:1,000; cat. no. ab134182; Abcam), focal adhesion kinase (FAK) (1:2,000; cat. no. ab40794; Abcam), p-FAK (1:1,000; cat. no. 81298; Abcam), multidrug resistance protein 1 (MRP1) (1:1,000; cat. no. ab260038; Abcam), breast cancer resistance protein (BCRP) (1:1,000; cat. no. ab207732;

Abcam), P-gp (1:2,000; cat. no. ab170904; Abcam) and β-actin (1:5,000; cat. no. ab6276; Abcam) at 4˚C. The membranes were then treated with secondary antibodies Goat Anti-Rabbit IgG H&L (HRP) (1:10,000; cat. no. ab6721; Abcam) or Goat Anti-Mouse IgG H&L (HRP) (1:10,000; cat. no. ab6789; Abcam) for 2 h at room temperature. Protein signals were recorded using a chemiluminescence (ECL) detection system (Solarbia S&T Co., Ltd.). The resulting images were assessed using an imaging system (Bio-Rad Laboratories, Inc.) and analyzed by a densitometric analysis software (Image Lab v3.0; Bio-Rad Laboratories, Inc.).

Sphere-formation assay. Single-cell suspensions were plated in ultralow attachment six-well plates (Corning, Inc.) at $5x10^3$ cells/ml and cultured in modified DMEM without serum supplementation, as described in the *Cell lines and cell culture* subsection. Media were replaced every 3 days. Cell spheres in each group were observed after 7 days.

ELISA. The levels of enzymes were evaluated using standardized commercially available kits. The following ELISA assay kit were purchased from Shanghai Yaji Biological Technology Co., Ltd.: VEGFR1 (cat. no. YS01065B), VEGFR2 (cat. no. YS06892B), VEGFR3 (cat. no. YS06893B), and C-Kit (cat. no. YS02312B). The EGFR ELISA assay kit (cat. no. H032) was bought from Nanjing Jiancheng Bioengineering institute. The following kits and antibodies were purchased from Merck KGaA: RET (cat. no. RAB0987), Flt-3 (cat. no. RAB1464), ErbB2 (cat. no. RAB0173k), ErbB4 (cat. no. RAB1041), FAK (cat. no. RAB095), FGFR1 (cat. no. RAB0961), FGFR2 (cat. no. RAB0962). PDGFR-α antibody (cat. no. SAB4502139), PDGFR-β antibody (cat. no. SAB4502148), SRC antibody (cat. no. SAB4502846), FGFR3 antibody (cat. no. SAB4500888) and FGFR4 antibody (cat. no. SAB1300137).

Molecular docking. AutoDock Vina v1.1.2 (http://vina.scripps.edu/) was used to determine ligands and the proteins required for molecular docking. The crystal structures of target proteins were obtained from the PDB database (https://www.rcsb.org/). The process involved a pre-treatment step, including hydrogen removal, amino acid modification, energy optimization and force field parameter adjustment. Subsequently, the retrieved ligand structure of luteolin (https://pubchem.ncbi.nlm.nih.gov/) was docked with the active sites of target proteins using the vina built-in pyrx software (https://pyrx.sourceforge.io/), with the affinity (kcal/mol) representing the combining capacity. Lower the affinity value, the more stable the ligand binding to the receptor. Visual analysis was performed using PyMOL (https://pymol.org/2/) and the two-dimensional figures were visualized using the Discovery Studio 2020 Client (https://discover.3ds.com/discovery-studio-visualizer-download).

Tumor xenografts in nude mice. A total of 25 female 4-6 weeks old athymic BALB/c nude mice (15-20 g) were obtained from Beijing Vital River Laboratory Animal Technology Co., Ltd. The animals were previously administered conventional feed, provided with *ad libitum* access to water and housed (temperature, 20-25˚C; humidity, 40-60%; 12-h light/dark cycle). In this research, mice was divided into four groups (NC, LUT, PTX and PTX + LUT) and anesthetized with 1% pentobarbital sodium. The mice in each group were injected with $2x10^6$ (200 μl) transfected EC1/PTX cells subcutaneously in the dorsal surface of the right hind leg to establish xenografts as the NC group. After inoculation, the mice were injected intraperitoneally with luteolin (20 or 40 mg/kg every day) in the LUT group, PTX (10 mg/kg every 3 days) in the PTX group and both drugs in the PTX + LUT group. The tumor size and weight were recorded. After 22 days, the mice were sacrificed by cervical dislocation and the tumor tissues were resected, imaged, weighed and measured.

Hematoxylin and eosin (H&E) staining. The tumor tissues were excised, immersed immediately in 10% formaldehyde and maintained at room temperature for 24 h. The tissues were dehydrated in 70, 80, 90, 95% alcohol for 30 min respectively, and then in anhydrous alcohol for 60 min for thorough dehydration. The tissues were embedded in pure paraffin and cut into 4 μm sections. The dehydrated tissue blocks were placed in xylene for 60 min for transparent treatment to facilitate paraffin penetration. The whole morphology was evaluated after H&E. staining at room temperature for 24 h. The stained sections were observed under an optical microscope (BX60; Olympus Corporation). Images were acquired and analysis was performed using ImageJ v1.8.0 Launcher (National Institutes of Health).

TUNEL staining. TUNEL staining was performed to assess apoptosis in tumor tissues at 37˚C within 30 min. Tissue slices were stained using an *in-situ* cell death detection kit (Roche Diagnostics) according to the manufacturer's instructions. The percentage of TUNEL-positive nuclei (green nuclei) was calculated.

Kyoto Encyclopedia of Genes and Genomes (KEGG) and Gene Ontology (GO) analysis. RStudio v3.6.1 (https://cloud.r-project.org/) was used to visualize GO terms and KEGG pathways. $P<0.05$ was set as the cutoff criterion for significant enrichment.

Statistical analysis. Statistical analysis was performed using the SPSS 21.0 software (IBM Corp.). Data from the experimental results are expressed as mean ± standard deviation (SD). The data were statistically analyzed using Independent samples t-test in 2 groups and one-way analysis of variance (ANOVA) followed by Tukey's post hoc test was used for ≥3 groups. $P<0.05$ was considered to indicate a statistically significant difference.

Results

The inhibitory effects of PTX on the proliferation of EC1 and EC1/PTX cells. The present study successfully established PTX-resistant human esophageal squamous cell carcinoma cells (EC1/PTX). As shown in Fig. 1A, the IC_{50} values of PTX in EC1 cells were 0.053±0.001 and 0.030±0.001 μg/ml at 24 and 48 h after PTX treatment, respectively. Meanwhile, the IC_{50} values of PTX in EC1/PTX cells were 0.914±0.044 and 0.540±0.014 μg/ml (Fig. 1B), respectively. The aforementioned

Table I. PTX for IC_{50} value in EC1and EC1/PTX cells.

	PTX/IC_{50} (mean ± SD, μg/ml)			
Time	EC1	EC1/PTX	RI	P-value
24 h	0.053±0.001	0.914±0.044	17.387	<0.01
48 h	0.030±0.001	0.540±0.014	17.834	<0.001

PTX, paclitaxel; RI, resistance index.

Table II. Luteolin for IC_{50} value in EC1and EC1/PTX cells.

	LUT/IC_{50} (mean ± SD, mmol/l)	
Cell lines	24 h	48 h
EC1	61.692±1.048	29.694±0.997
EC1/PTX	64.875±1.447	32.457±1.104

PTX, paclitaxel.

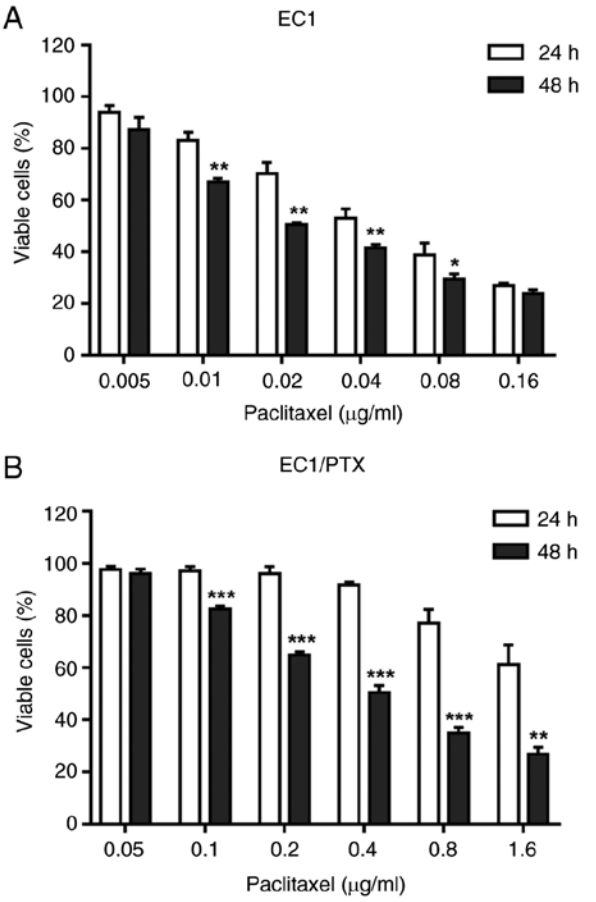

Figure 1. The effects of PTX on the proliferation of EC1 and EC1/PTX cells. (A) The inhibitory effects of PTX at different concentrations (0.005, 0.01, 0.02, 0.04, 0.08, 0.16 μg/ml) on the proliferation of EC1 cells. (B) The inhibitory effects of PTX at different concentrations (0.05, 0.1, 0.2, 0.4, 0.8, 0.16 μg/ml) on the proliferation of EC1/PTX cells. *P<0.05, **P<0.01, ***P<0.001 vs. DMSO. PTX, paclitaxel.

results indicated that PTX exerted a certain inhibitory effect on the proliferation of parental and resistant cells. The resistance indexes (RIs) were 17.387 at 24 h and 17.834 at 48 h, respectively (Table I).

Luteolin inhibits proliferation but induced cell cycle arrest and apoptosis in PTX-resistant ESCC cells. The present study used luteolin at different concentrations (10, 20, 40, 80 and 120 μM) to treat parental cells (EC1) and PTX-resistant ESCC cells (EC1/PTX) and calculated the IC_{50} values of luteolin while determining the cell survival rate. The IC_{50} values of luteolin in EC1 cells were 61.692±1.048 and 29.694±0.997 μM after treatment for 24 and 48 h, respectively. Meanwhile, in the EC1/PTX cells, the IC_{50} values were 64.875±1.447 and 32.457±1.104 μM, respectively. Notably, the viability of EC1 and EC1/PTX cells was inhibited by luteolin in a time- and dose-dependent manner (Fig. 2A and Table II).

To detect luteolin-induced changes in the biological function of PTX-resistant cells, 10, 20 and 40 μM luteolin was used to treat EC1/PTX cells. Cloning and flow cytometry assays were used to assess clone formation, cell cycle progression and apoptosis. As shown in Fig. 2B, luteolin (10, 20 and 40 μM) could significantly inhibit colony formation in a dose-dependent manner. The clonogenic capacities were 138.55±6.32% in the DMSO group, 80.01±2.92% in the 10 μM luteolin group, 52.76±2.54% in the 20 μM luteolin group and 16.71±3.34% in the 40 μM luteolin group. In addition, compared to that in the DMSO group, luteolin treatment significantly increased the total apoptosis rate (including that of cells in early and late apoptosis) in a dose-dependent manner (Fig. 2C) and induced cell cycle distribution in the G_2/M phase (Fig. 2D).

Luteolin suppresses the migration, invasion, epithelial-mesenchymal transition (EMT) and dry spheroidization of PTX-resistant ESCC cells. The present study used 10 and 20 μM luteolin to treat EC1/PTX cells and examined the migration and invasion potential of resistant cells in the wound healing and Transwell assays, individually. The cell migration rate (Fig. 3A) and number of transmembrane cells (Fig. 3B) in the luteolin administration group were significantly lesser than those in the DMSO group. TGF-β1 is widely used to induce EMT in cells. The present study co-treated the cells with 10 ng/ml TGF-β1 and 10 or 20 μM luteolin and determined the expression level of EMT-related proteins in the cells by western blotting. TGF-β1 induced the expression of Snail, N-cadherin and MMP-2 proteins, which was downregulated upon luteolin treatment (Fig. 3C). Subsequently, a cell microsphere formation experiment was conducted to assess the spheroidization of cells and expression for stem cell markers. Compared with luteolin-treated cells, which formed smaller microspheres and had more debris, DMSO-treated cells formed larger microspheres and exhibited more rapid proliferation (Fig. 3D). Besides, the expression of stem cell markers (SOX-2, CD44 and CD133) was significantly downregulated upon luteolin treatment (Fig. 3E).

Luteolin enhances drug sensitivity and, combined with PTX, facilitates apoptosis in drug-resistant ESCC cells. Luteolin (10, 20 and 40 μM) was used to treat EC1/PTX cells for 24 h. At

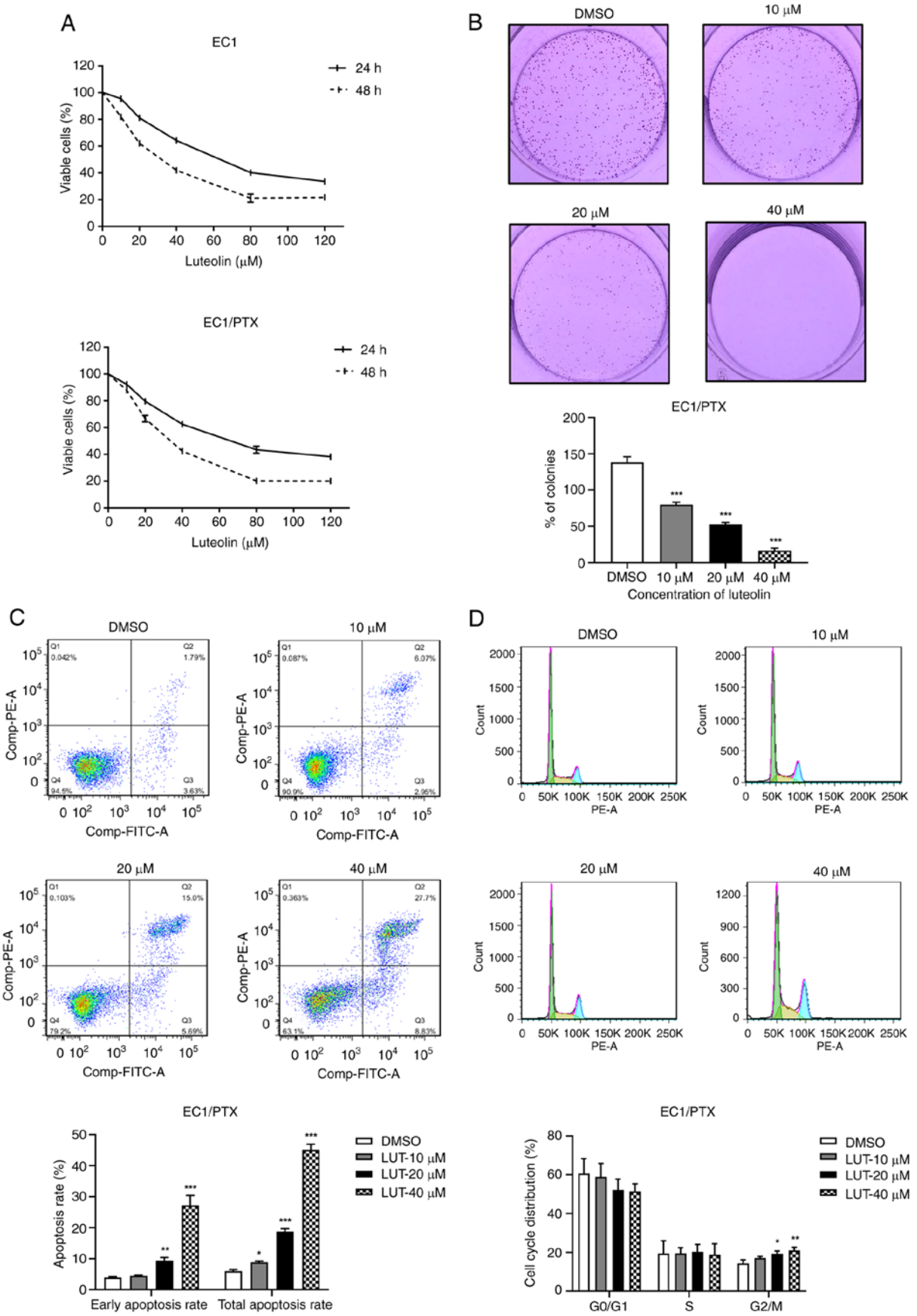

Figure 2. Effects of luteolin on cell proliferation, cell cycle and apoptosis in PTX-resistant ESCC cells. (A) The inhibitory effects of luteolin at different concentrations (10, 20, 40, 80 and 120 μM) on the proliferation of EC1 cells and EC1/PTX drug-resistant cells. (B) Luteolin (10, 20 and 40 μM) exerted its effects on EC1/PTX cells. After 7 days, the cells were stained with 0.1% crystal violet solution and clone proliferation was analyzed. (C) Luteolin (10, 20 and 40 μM) acted on EC1/PTX cells for 48 h. The apoptosis rate of cells in different treatment groups was determined by flow cytometry after Annexin-FITC/PI staining. (D) Luteolin (10, 20 and 40 μM) was used to treat EC1/PTX cells for 24 h and cell cycle distribution was determined by flow cytometry after PI staining. *P<0.05, **P<0.01, ***P<0.001 vs. DMSO n=3. PTX, paclitaxel; ESCC, esophageal squamous cell carcinoma.

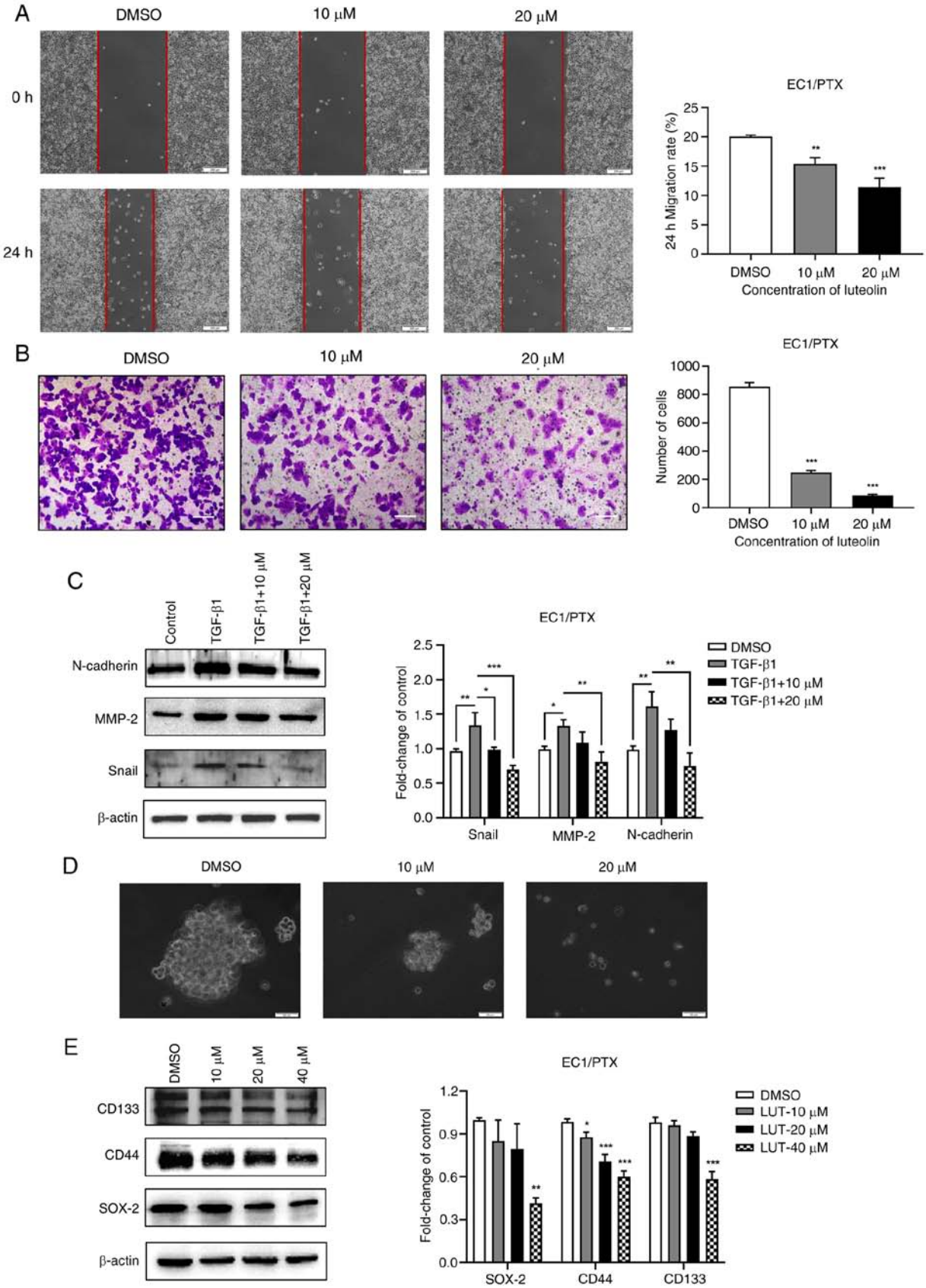

Figure 3. Effects of luteolin on the migration, invasion, EMT and dry spheroidization of PTX-resistant ESCC cells. (A) Wound healing assay was used to evaluate the inhibitory effect of luteolin on the migration potential of EC1/PTX cells (magnification, x200). (B) A Transwell chamber was used to determine the inhibitory effect of luteolin on the invasion potential of EC1/PTX cells (magnification, x100). (C) TGF-β1 was used to induce EMT in EC1/PTX cells and the cells were treated with 10 or 20 μM luteolin. The expression levels of EMT-related proteins were determined by western blotting. (D) A cell microsphere formation test was performed to determine the effect of luteolin on the spheroidizing potential of EC1/PTX cells (magnification, x50). (E) After EC1/PTX cells were treated with luteolin at different concentrations (10, 20 and 40 μM) for 24 h, western blotting was performed to determine the expression levels of stem cell markers in the cells. *P<0.05, **P<0.01, ***P<0.001 vs. DMSO n=3. EMT, epithelial-mesenchymal transition; PTX, paclitaxel; ESCC, esophageal squamous cell carcinoma.

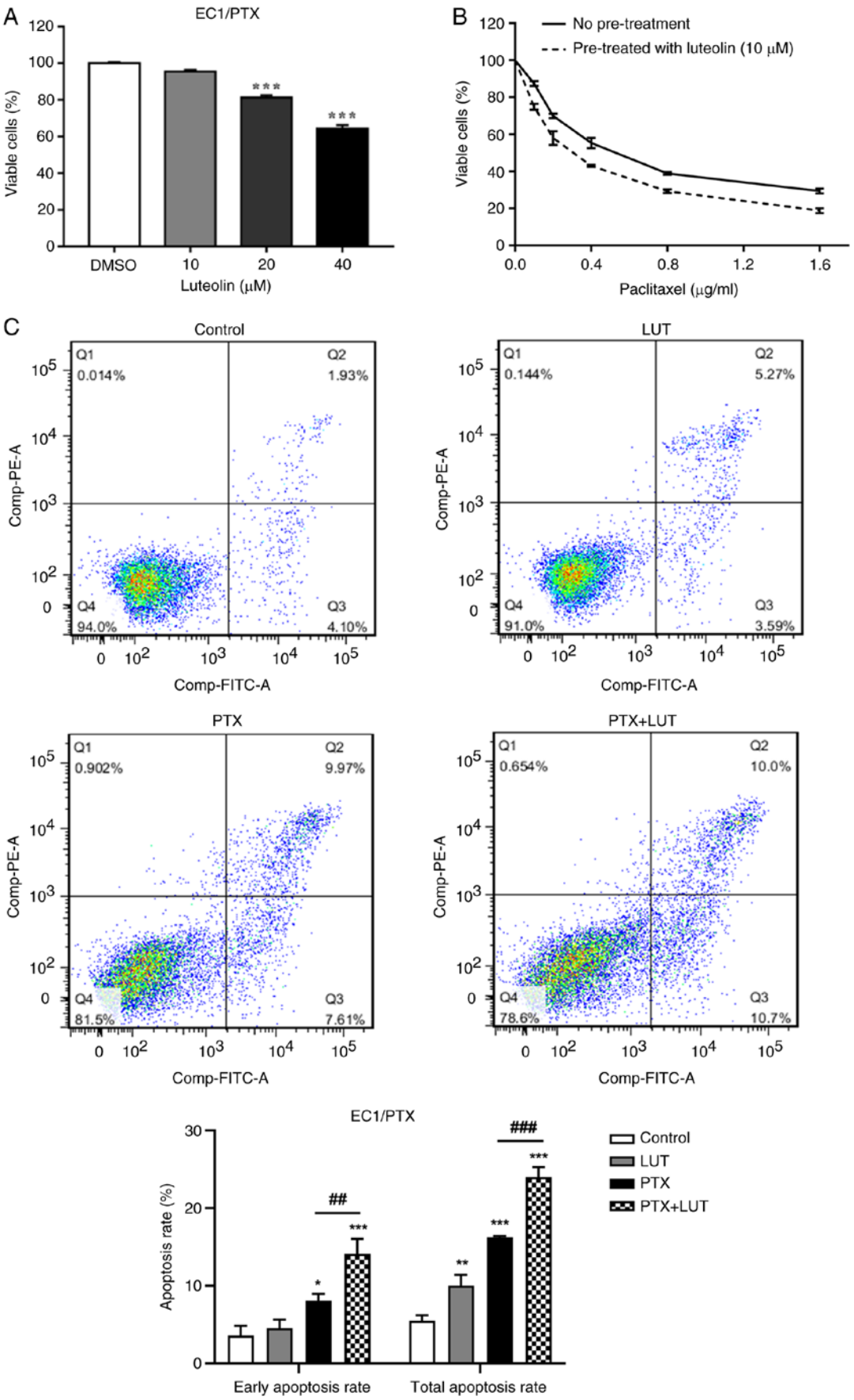

Figure 4. A combination of luteolin and PTX increased drug sensitivity and apoptosis in PTX-resistant ESCC. (A) The survival rate of EC1/PTX cells after 24 h of treatment with luteolin (10, 20 and 40 μM). (B) The effects of luteolin on the PTX sensitivity of EC1/PTX cells. ***P<0.001 vs. DMSO. (C) Luteolin, PTX and luteolin plus PTX were used to treat EC1/PTX cells for 48 h. After Annexin-FITC/PI staining, the apoptosis rate of cells in the different treatment groups was determined by flow cytometry. *P<0.05, **P<0.01, ***P<0.001 vs. Control, $^{\#\#}$P<0.01, $^{\#\#\#}$P<0.001 vs. PTX, n=3. PTX, paclitaxel; ESCC, esophageal squamous cell carcinoma.

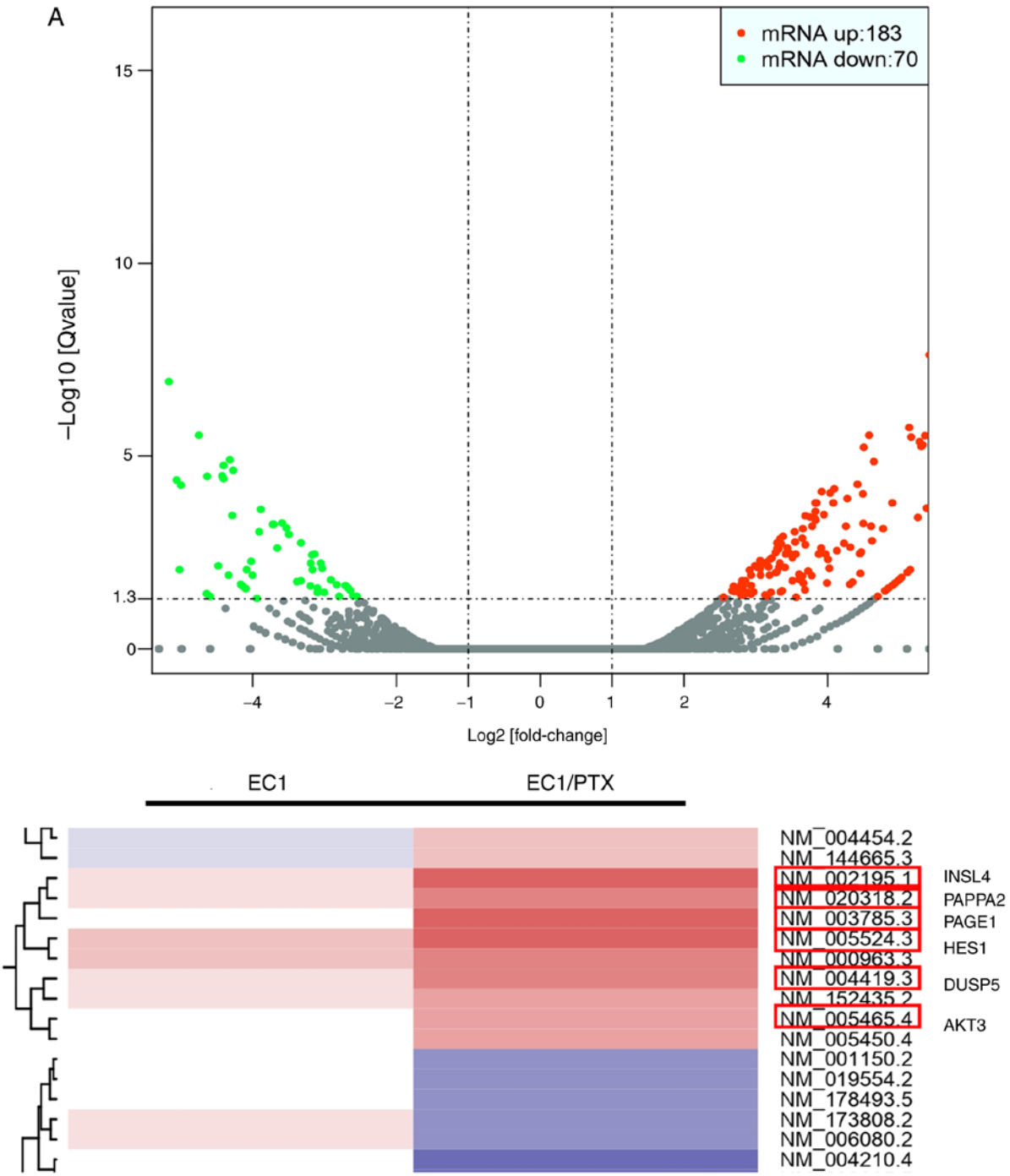

Figure 5. Continued.

concentrations of 20 and 40 μM, luteolin significantly reduced cell growth (Fig. 4A). Based on its low cytotoxicity, 10 μM luteolin was selected for subsequent experiments. The IC_{50} value of PTX in EC1/PTX cells decreased from 0.560±0.026 to 0.366±0.007 μM upon luteolin pretreatment, a reduction by 1.5 folds (Fig. 4B). Next, 10 μM luteolin and 0.2 μg/ml PTX was used individually and in combination to treat EC1/PTX cells. Cells were then examined by flow cytometry following Annexin-FITC/PI staining. The total apoptosis rates were 5.50±0.58, 10.05±1.11, 16.23±0.16 and 24.00±1.04% in the Control, LUT, PTX and PTX + LUT groups, respectively. Compared to that in the LUT group or PTX group, the total apoptosis rate in the PTX + LUT group was significantly higher (Fig. 4C).

The PI3K/Akt signaling pathway may be involved in PTX-resistant ESCC. To explore the mechanism underlying the reversal of drug resistance in EC1/PTX cells by luteolin, whole-transcriptome next-generation sequencing was performed on parental and drug-resistant cells to screen RNA exhibiting differentiated expression. High-throughput sequencing analysis was performed to obtain the Volcano plot and heatmap. These plots showed the differential expression of mRNAs. Compared to the parent cells, PTX-resistant

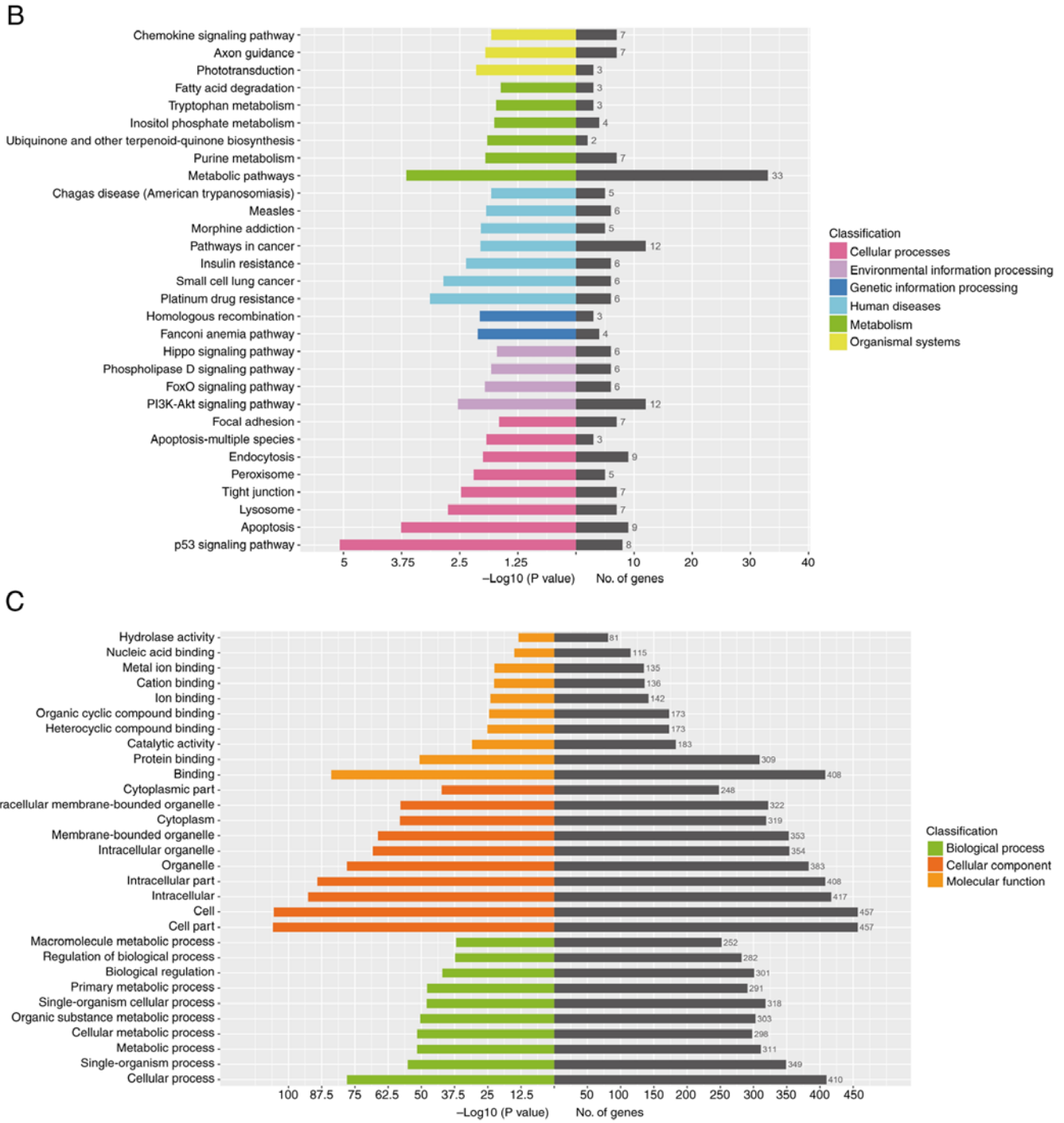

Figure 5. KEGG and GO analysis of the aberrant expression of genes. (A) A heatmap and volcano map were prepared by next-generation sequencing. (B) KEGG biological pathway enrichment analysis. (C) GO gene function enrichment analysis. KEGG, Kyoto Encyclopedia of Genes and Genomes; GO, Gene Ontology.

ESCC cells showed 253 abnormally expressed mRNA molecules, of which 183 were upregulated, whereas 70 were downregulated. Among these, AKT3, INSL4, PAPPA2, PAGE1, HES1 and DUSP5 mRNAs showed significant upregulation, which was accompanied by a multiple of difference $\log_2$ (fold change) >3.00 (Fig. 5A). This suggested that AKT3, as a key molecule in the PI3K/Akt signaling pathway, may be significantly upregulated in PTX-resistant ESCC cells. Following this, Kyoto Encyclopedia of Genes and Genomes biological pathway enrichment analysis was performed using the differentially expressed genes. The results showed that certain signaling pathways, including the PI3K/Akt, p53, apoptosis and metabolism-related pathways, among others, were closely associated with drug resistance in ESCC cells (Fig. 5B). Furthermore, the Gene Ontology enrichment analysis results showed that the changes (signal transduction, apoptosis, cell metabolism and other functions) were significantly associated with PTX resistance (Fig. 5C). This finding suggested that the PI3K/Akt signaling pathway may be involved in PTX resistance in ESCC cells. Subsequently, the inhibitory activity of luteolin on tyrosine kinases was screened using ELISA. Each tyrosine

Table III. Inhibition rate of tyrosine kinase activity (%).

	Inhibition rate of different concentration (nM) compounds on tyrosine kinase activity (%)													
	Luteolin				SU11248		BIBW2992		Dasatinib		PF562271		PF562271	
Kinases	1,000	SD	100	SD	1,000	SD	1,000	SD	1,000	SD	1,000	SD	1,000	SD
VEGFR-1	81.4	5.1	18.8	13.2	90.8	3.8								
VEGFR-2	70.9	6.8	31.1	4.1	95.1	0.9								
VEGFR-3	99.9	0.2	37.8	8.0	99.9	0.1								
PDGFR-α	57.1	15.3	65.5	11.7	92.7	4.1								
PDGFR-β	73.4	4.2	43.5	6.2	92.2	1.9								
RET	99.9	0.2	45.7	7.4	99.8	0.3								
C-Kit	99.7	0.5	63.1	2.6	99.7	0.7								
Flt-3	91.2	6.0	56.9	15.3	99.9	0.2								
EGFR	84.9	3.6	25.6	17.2			100.0	0.1						
ErbB2	**100.0**	**0.0**	**62.0**	**21.0**			**97.1**	**5.9**						
ErbB4	91.2	2.1	33.0	7.1			100.0	0.0						
Src	**57.4**	**18.3**	**2.1**	**2.5**					**99.8**	**0.3**				
FAK	**76.1**	**9.7**	**42.4**	**20.4**							**99.2**	**0.8**		
FGFR1	94.6	6.3	35.0	11.8									100.0	0.0
FGFR2	86.5	4.6	72.1	6.5									100.0	0.0
FGFR3	82.0	8.7	8.6	14.6									100.0	0.0
FGFR4	77.5	1.3	46.3	8.5									98.4	0.5

Figures in bold are the key kinases of the FAK/Src/PI3K/Akt pathway. FAK, focal adhesion kinase.

kinase-specific inhibitor was used as a control. Luteolin inhibited the activities of various tyrosine kinases, which included FAK, ErbB2 and Src kinase. The rates of inhibition of FAK, Src and ErbB2 activities upon treatment with 1,000 nM luteolin were 76.1±9.7, 57.4±18.3 and 100.0±0.0%, respectively (Table III). Thus, luteolin can inhibit key kinases in the FAK/Src/PI3K/Akt signaling pathway.

Luteolin reduces the expression of associated proteins of the FAK/Src/PI3K/Akt pathway and resistance-related proteins. To evaluate whether luteolin could reverse PTX-induced resistance by regulating the PI3K/Akt signaling pathway, EC1/PTX cells were treated with 10, 20 and 40 μM luteolin and the expression of associated proteins in the FAK/Src/PI3K/Akt pathway and resistance-related proteins was measured. Compared to that in the DMSO group, the expression of p-FAK (Tyr397)/FAK, ErbB2, p-Src (Tyr416)/Src and p-Akt (Ser473)/Akt was significantly downregulated in the luteolin-treated group (Fig. 6A). A similar tendency was observed in the expression of the drug-resistance-related proteins P-gp, BCRP and MRP1 (Fig. 6B).

Luteolin can bind to the active sites of FAK, SRC and AKT. Luteolin was linked to the active sites of FAK, SRC and AKT. Luteolin formed hydrogen bonds with THR152, GLU162, HIS211, HISS204 and LYS198 in SRC (1A07), with a binding energy of -7.7 kcal/mol (Fig. 7A). Luteolin formed hydrogen bonds with HIS89 in AKT (1H10). Meanwhile, it showed hydrophobic interactions with the residues HIS13, TRP11

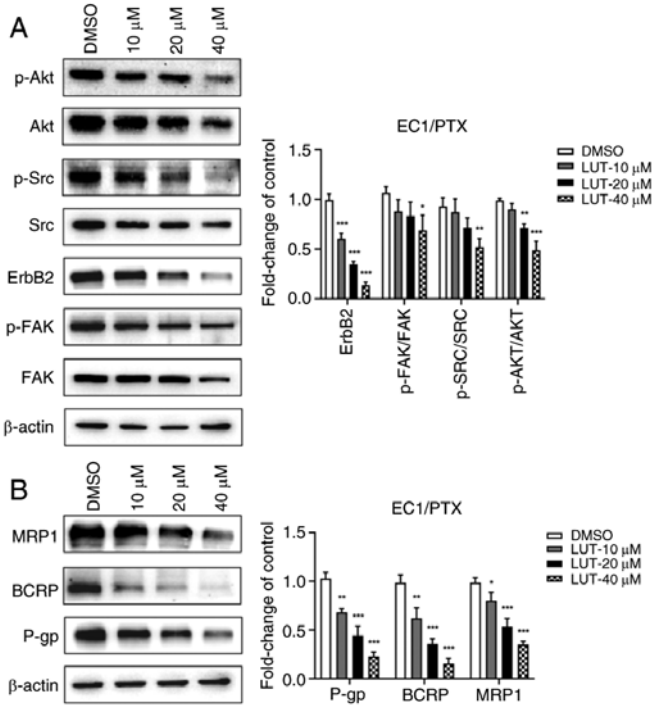

Figure 6. The expression patterns of proteins associated with the FAK/Src/PI3K/Akt pathway and PTX resistance in ESCC cells. Luteolin (10, 20 and 40 μM) was used to treat EC1/PTX cells for 24 h. (A) Proteins associated with the FAK/Src/PI3K/Akt pathway were detected by western blotting. (B) Drug resistance-associated proteins were detected by western blotting. *P<0.05, **P<0.01, ***P<0.001 vs. DMSO n=3. FAK, focal adhesion kinase; PTX, paclitaxel; ESCC, esophageal squamous cell carcinoma; p-, phosphorylated; MRP1, multidrug resistance protein 1; BCRP, breast cancer resistance protein.

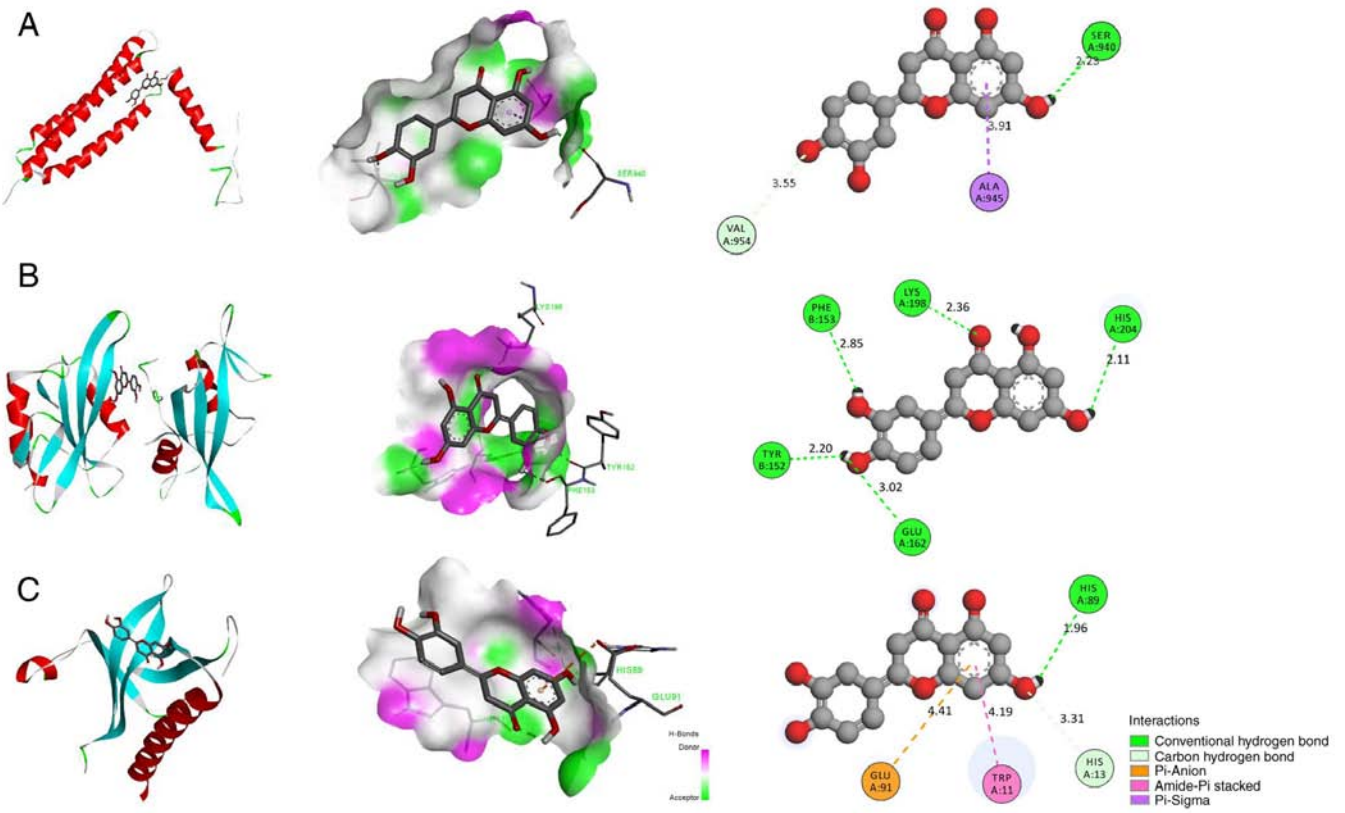

Figure 7. Visualization of the molecular docking of luteolin with target proteins. Molecular modeling was used to dock luteolin into the binding sites of (A) FAK, (B) Src and (C) AKT. FAK, focal adhesion kinase.

and GLU91, with a binding energy of -6.2 kcal/mol (Fig. 7B). Luteolin formed hydrogen bonds with SER940 in FAK (1K04) and formed hydrophobic bonds with ALA945 and VAL954, with a binding energy of -6.6 kcal/mol (Fig. 7C). The lower the binding energy, the higher the docking effect. Collectively, the results indicated that luteolin had a strong binding ability to the active sites of FAK, SRC and AKT.

Luteolin combined with PTX inhibits tumorigenesis in xenografts in nude mice in vivo. To explore the sensitization effects of luteolin *in vivo*, a nude mouse xenograft model was developed using EC1/PTX cells. Each group of cells was treated with 0.9% v/v NS, 20 mg/kg luteolin, 40 mg/kg luteolin, 10 mg/kg PTX and 10 mg/kg PTX + 20 mg/kg luteolin. As shown in Fig. 8A, the body weight of nude mice in each group increased marginally during the treatment period, but there were no significant differences in the body weights of mice between the treatment and NC groups. The tumor volume in the NC group increased rapidly, whereas the tumor growth rate in the luteolin group or PTX group was relatively slow and the tumor growth rate in the PTX + LUT-20 mg/kg group was the slowest (Fig. 8B). From the 16th to the 22nd day of treatment, the tumor volume in the luteolin or PTX group was significantly reduced compared with that in the NC group and the tumor volume in the combination group was the lowest. After 22 days of treatment, the average tumor mass in the PTX group and LUT-40 mg/kg group was significantly smaller than that in the NC group. The value showed no significant difference from that in the LUT-20 mg/kg group and showed no obvious toxicity *in vivo*. Compared with the two single-treatment groups, the combined treatment group had a significantly lower average tumor mass (Fig. 8C-D). H&E staining showed that tumor cells in the NC and LUT groups were uniformly stained and arranged regularly and densely, exhibiting a clear clumping growth trend. By contrast, tumor cells in the PTX and PTX + LUT groups had an irregular morphology, with the nuclear chromatin being partially dense and concentrated with nuclear pyknosis. The degree of apoptosis in the PTX + LUT group was the highest among the four groups (Fig. 8E). In addition, the TUNEL-positive area with green fluorescence in the PTX + LUT group was considerably larger than that in the PTX group (Fig. 8F). Thus, combined treatment with luteolin and PTX led to a synergistic effect on the inhibition of drug resistance in EC1 cells *in vivo*.

Luteolin suppresses the expression of FAK/Src/PI3K/Akt pathway and resistance-related proteins in vivo. The expression of p-FAK (Tyr397)/FAK, ErbB2, p-Src (Tyr416)/Src and p-Akt (Ser473)/Akt (Fig. 9A) and resistance proteins (P-gp, BCRP and MRP1) (Fig. 9B) was significantly downregulated in a dose-dependent manner in response to luteolin treatment. These results suggested that luteolin may reverse PTX resistance in cells by inhibiting the expression of drug-resistant proteins mediated by the FAK/Src/PI3K/Akt signaling pathway.

Discussion

Luteolin can inhibit the proliferation of various tumor cells *in vitro* and hinder tumor progression by inducing cell cycle

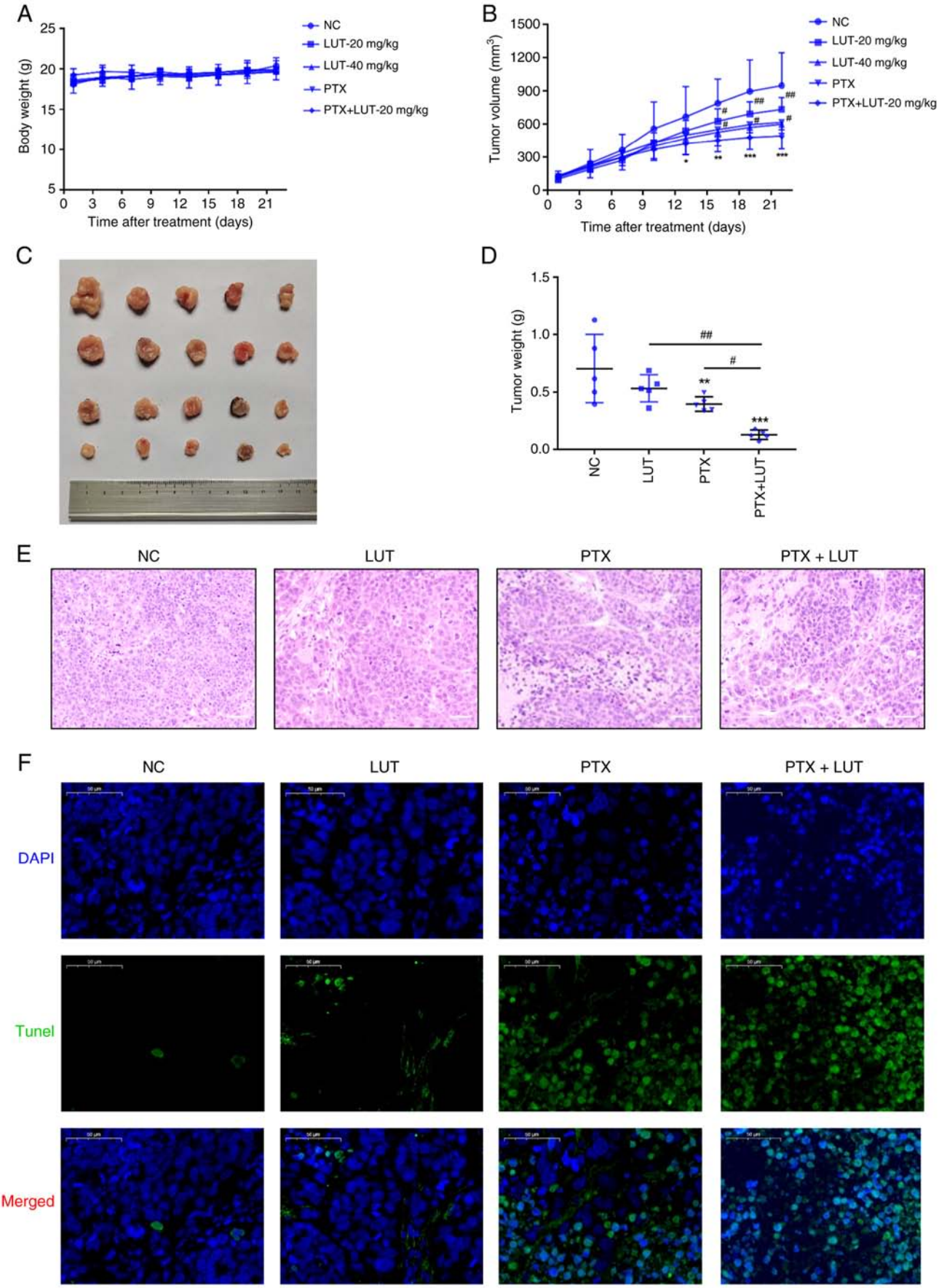

Figure 8. Effect of treatment with luteolin combined with PTX on the xenografts in nude mice and apoptosis *in vivo*. Luteolin combined with PTX was used to treat xenografts in nude mice. (A) The body weights of nude mice were measured. (B) The tumor volumes were measured. (C) The images of tumors were acquired. (D) The average tumor mass was measured. **P<0.01 vs. NC, $^{\#}$P<0.05 vs. 20 mg/kg, n=5. (E) Hematoxylin and eosin staining assay for cell morphology in different groups (magnification, x100). (F) TUNEL assay for apoptosis in different groups (magnification, x50). *P<0.05, **P<0.01, ***P<0.001 vs. NC, $^{\#}$P<0.05, $^{\#\#}$P<0.01 vs. PTX + LUT, n=5. PTX, paclitaxel; LUT, luteolin; NC, normal control.

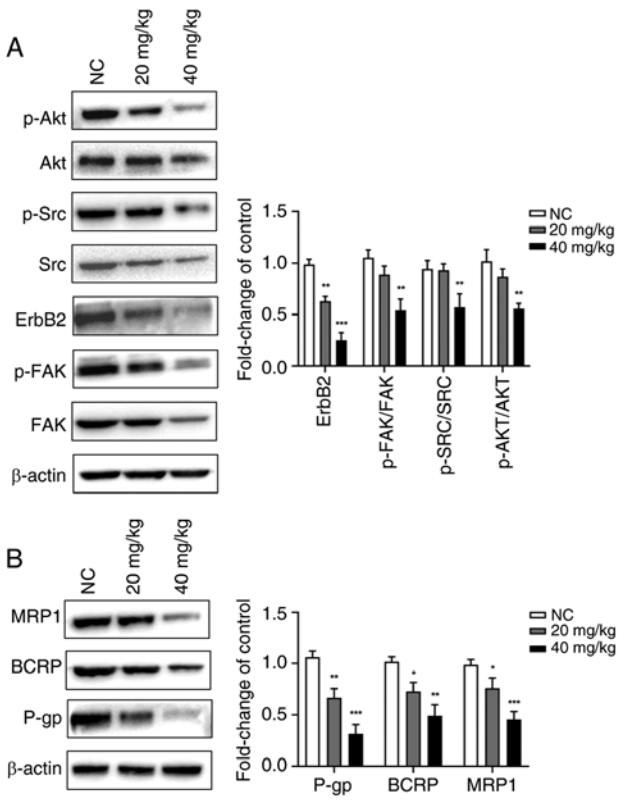

Figure 9. Effect of luteolin on the expression patterns of proteins associated with the FAK/Src/PI3K/Akt pathway and drug resistance *in vivo*. Luteolin (20 or 40 mg/kg) was used to treat xenografts in nude mice. (A) Proteins associated with the FAK/Src/PI3K/Akt pathway were detected by western blotting. (B) The resistance-associated proteins were detected by western blotting. *P<0.05, **P<0.01, ***P<0.001 vs. NC, n=3. FAK, focal adhesion kinase; PTX, paclitaxel; ESCC, esophageal squamous cell carcinoma; p-, phosphorylated; MRP1, multidrug resistance protein 1; BCRP, breast cancer resistance protein; NC, normal control.

arrest, facilitating apoptosis and inhibiting invasion, metastasis and angiogenesis. The present study examined the biological effects of luteolin on PTX resistance in ESCC cells. Luteolin inhibited proliferation, clone formation, migration, invasion and EMT in the cells but induced cell cycle arrest and apoptosis. It also reduced sphere formation and stemness in EC1/PTX cells.

In recent years, luteolin has been shown to play a vital role in chemotherapeutic sensitization by regulating the biological characteristics of drug-resistant tumor cells, thereby increasing the drug sensitivity in these cells and improving the therapeutic effect of cellular chemotherapeutics. For example, Tsai *et al* (19) showed that luteolin suppressed breast cancer stemness and enhanced chemosensitivity via an Nrf2-mediated pathway. In another study, luteolin combined with low-dose PTX synergistically restricted EMT and induced apoptosis in esophageal carcinoma *in vitro* and *in vivo*. Ma *et al* (20) showed that luteolin potentiated the oxaliplatin-induced inhibitory effects on cell proliferation in gastric cancer by inducing G_2/M cell cycle arrest and apoptosis. In the current study, luteolin treatment combined with PTX treatment significantly increased the total apoptosis rate compared to that achieved with PTX or luteolin administration. This suggested that luteolin, as an adjuvant, increased the chemosensitivity of PTX-resistant ESCC cells.

FAK is a type of non-receptor tyrosine kinase that can promote focal adhesion and EMT when phosphorylated, thereby regulating cell invasion and metastasis (21-22). ErbB2, also known as HER2, is a member of the epidermal growth factor receptor family of transmembrane tyrosine kinase receptors. The aberrant expression of ErbB2 usually contributes to malignant transformation and has been linked to cell invasion, lymph node metastasis, poor prognosis and chemotherapy tolerance (23,24). The activation of both ErbB2 (recruited by FAK) and FAK triggers Src (a non-receptor tyrosine kinase, encoded by the viral oncogene SRC) and the subsequent activation of Src downstream signaling pathways (e.g. PI3K/AKT and MAPK) induces tumor apoptosis, promoting tumor invasion, metastasis and chemoresistance. The next-generation sequencing results of ESCC drug-resistant cells (EC1/PTX) and its parental cells (EC1) were analyzed and it was found that a series of signaling pathways (e.g., PI3K/Akt, p53, apoptosis and metabolic pathways) and functional changes (signal transduction, apoptosis and cell metabolism) were significantly related to drug resistance. Meanwhile, among mRNAs exhibiting differential expression, AKT3, as the key molecule in the PI3K/Akt pathway, was significantly upregulated in drug-resistant ESCC cells.

Subsequently, based on its inhibitory effects on *in vitro* tyrosine kinase activity, luteolin can function as a multi-target kinase inhibitor owing to its ability to suppress the activity of multiple tyrosine kinases. Interestingly, the kinase activities of FAK, ErbB2 and Src could be inhibited to different degrees and luteolin could inhibit key kinases in the FAK/Src/PI3K/Akt pathway. This may be a crucial method for reversing drug resistance in ESCC.

The present study also assessed whether luteolin increased the chemotherapeutic drug sensitivity of drug-resistant ESCC cells by blocking the FAK/Src/PI3K/Akt signaling pathway. The results of the *in vivo* and *in vitro* experiments showed that luteolin restricted the expression levels of p-FAK (Tyr397)/FAK, ErbB2, p-Src (Tyr416)/Src, p-Akt (Ser473)/Akt, P-gp, BCRP and MRP1. This indicated that the FAK/Src/PI3K/Akt signaling pathway is involved in drug resistance in ESCC cells. Meanwhile, molecular docking and visualization experiments were performed using luteolin with FAK, SRC and AKT proteins from the PI3K-Akt signaling pathway. Luteolin exhibited good binding ability to the active sites of FAK, SRC and AKT. Therefore, luteolin may increase drug sensitivity in ESCC-resistant cells by inhibiting the FAK/Src/PI3K/Akt signaling pathway.

It was concluded that luteolin inhibits tumorigenesis in drug-resistant tumor cells potentially through modulation of the FAK/Src/PI3K/Akt signaling pathway. However, the present study had certain limitations. In future research, it is planned to validate its findings using different subtypes of drug-resistant ESCC cell lines and further investigate specific binding sites between luteolin and key kinases through molecular docking analysis. These results could serve as a foundation for considering luteolin as a clinical adjuvant and a promising agent for reversing drug resistance in ESCC cells.

Acknowledgements

Not applicable.

Funding

The present study was supported by the General program of Henan Natural Science Foundation (grant no. 212300410393), Henan Science and Technology Research Project (grant no. 232102310298) and Henan Province Medical Science and Technology Research Program Joint Construction Project (grant no. LHGJ20210696).

Availability of data and materials

The data generated in the present study may be requested from the corresponding author.

Authors' contributions

ZY and TF designed the study and wrote the first draft of the manuscript. HL revised the manuscript. TF, YS and NG conducted the bioinformatics analysis. ZY, PG and YH developed the methods and performed the validation. YL, YS and PG participated in data analysis and tabulation. NG and HL performed the statistical analysis. ZY and HL confirmed the authenticity of all the raw data. All authors read and approved the final manuscript.

Ethics approval and consent to participate

Not applicable.

Patient consent for publication

Not applicable.

Competing interests

The authors declare that they have no competing interests.

References

1. Bray F, Ferlay J, Soerjomataram I, Siegel RL, Torre LA and Jemal A: Global cancer statistics 2018: GLOBOCAN estimates of incidence and mortality worldwide for 36 cancers in 185 countries. CA Cancer J Clin 68: 394-424, 2018.
2. Zhang Y: Epidemiology of esophageal cancer. World J Gastroenterol 19: 5598-5606, 2013.
3. Abnet CC, Arnold M and Wei WQ: Epidemiology of esophageal squamous cell carcinoma. Gastroenterology 154: 360-373, 2018.
4. Siegel R, Naishadham D and Jemal A: Cancer statistics, 2013. CA Cancer J Clin 63: 11-30, 2013.
5. Lin Y, Totsuka Y, He Y, Kikuchi S, Qiao Y, Ueda J, Wei W, Inoue M and Tanaka H: Epidemiology of esophageal cancer in Japan and China. J Epidemiol 23: 233-242, 2013.
6. Hiripi E, Jansen L, Gondos A, Emrich K, Holleczek B, Katalinic A, Luttmann S, Nennecke A and Brenner H; Gekid Cancer Survival Working Group: Survival of stomach and esophagus cancer patients in Germany in the early 21st century. Acta Oncol 51: 906-914, 2012.
7. van Hagen P, Hulshof MC, van Lanschot JJ, Steyerberg EW, van Berge Henegouwen MI, Wijnhoven BP, Richel DJ, Nieuwenhuijzen GA, Hospers GA, Bonenkamp JJ, *et al*: Preoperative chemoradiotherapy for esophageal or junctional cancer. N Engl J Med 366: 2074-2084, 2012.
8. Gebski V, Burmeister B, Smithers BM, Foo K, Zalcberg J and Simes J; Australasian Gastro-Intestinal Trials Group: Survival benefits from neoadjuvant chemoradiotherapy or chemotherapy in oesophageal carcinoma: A meta-analysis. Lancet Oncol 8: 226-234, 2007.
9. Ando N, Kato H, Igaki H, Shinoda M, Ozawa S, Shimizu H, Nakamura T, Yabusaki H, Aoyama N, Kurita A, *et al*: A randomized trial comparing postoperative adjuvant chemotherapy with cisplatin and 5-fluorouracil versus preoperative chemotherapy for localized advanced squamous cell carcinoma of the thoracic esophagus (JCOG9907). Ann Surg Oncol 19: 68-74, 2012.
10. Liu Y, Ren Z, Yuan L, Xu S, Yao Z, Qiao L and Li K: Paclitaxel plus cisplatin vs. 5-fluorouracil plus cisplatin as first-line treatment for patients with advanced squamous cell esophageal cancer. Am J Cancer Res 6: 2345-2350, 2016.
11. Hummel R, Sie C, Watson DI, Wang T, Ansar A, Michael MZ, Van der Hoek M, Haier J and Hussey DJ: MicroRNA signatures in chemotherapy resistant esophageal cancer cell lines. World J Gastroenterol 20: 14904-1412, 2014.
12. Limtrakul P, Anuchapreeda S and Buddhasukh D: Modulation of human multidrug-resistance MDR-1 gene by natural curcuminoids. BMC Cancer 4: 13, 2004.
13. Lopez-Lazaro M: Distribution and biological activities of the flavonoid luteolin. Mini Rev Med Chem 9: 31-59, 2009.
14. Shi R, Huang Q, Zhu X, Ong YB, Zhao B, Lu J, Ong CN and Shen HM: Luteolin sensitizes the anticancer effect of cisplatin via c-Jun NH2-terminal kinase-mediated p53 phosphorylation and stabilization. Mol Cancer Ther 6: 1338-1347, 2007.
15. Chian S, Li YY, Wang XJ and Tang XW: Luteolin sensitizes two oxaliplatin-resistant colorectal cancer cell lines to chemotherapeutic drugs via inhibition of the Nrf2 pathway. Asian Pac J Cancer Prev 15: 2911-2916, 2014.
16. Pandurangan AK, Dharmalingam P, Sadagopan SK and Ganapasam S: Luteolin inhibits matrix metalloproteinase 9 and 2 in azoxymethane-induced colon carcinogenesis. Hum Exp Toxicol 33: 1176-1185, 2014.
17. Carsten VF and Cardinale PJ: The overdenture-a review. N Y State Dent J 44: 331-334, 1978.
18. Wu YT, Chen L, Tan ZB, Fan HJ, Xie LP, Zhang WT, Chen HM, Li J, Liu B and Zhou YC: Luteolin inhibits vascular smooth muscle cell proliferation and migration by inhibiting TGFBR1 signaling. Front Pharmacol 9: 1059, 2018.
19. Tsai KJ, Tsai HY, Tsai CC, Chen TY, Hsieh TH, Chen CL, Mbuyisa L, Huang YB and Lin MW: Luteolin inhibits breast cancer stemness and enhances chemosensitivity through the Nrf2-mediated pathway. Molecules 26: 6452, 2021.
20. Ma J, Chen X, Zhu X, Pan Z, Hao W, Li D, Zheng Q and Tang X: Luteolin potentiates low-dose oxaliplatin-induced inhibitory effects on cell proliferation in gastric cancer by inducing G2/M cell cycle arrest and apoptosis. Oncol Lett 23: 16, 2022.
21. Lee BY, Timpson P, Horvath LG and Daly RJ: FAK signaling in human cancer as a target for therapeutics. Pharmacol Ther 146: 132-149, 2015.
22. Seguin L, Desgrosellier JS, Weis SM and Cheresh DA: Integrins and cancer: Regulators of cancer stemness, metastasis and drug resistance. Trends Cell Biol 25: 234-240, 2015.
23. Vadlamudi RK, Sahin AA, Adam L, Wang RA and Kumar R: Heregulin and HER2 signaling selectively activates c-Src phosphorylation at tyrosine 215. FEBS Lett 543: 76-80, 2003.
24. Yu D and Hung MC: Overexpression of ErbB2 in cancer and ErbB2-targeting strategies. Oncogene 19: 6115-6121, 2000.